DELPHI Collaboration

DELPHI 2006-008 CONF 754
12 July, 2006

Observation of the inner muon bremsstrahlung in dimuon events at LEP1

A.Ferrer, V.F. Perepelitsa
Valencia University/ITEP

Abstract

Muon bremsstrahlung photons converted in front of the DELPHI main tracker (TPC) in dimuon events at LEP1 were studied in the the kinematic range of $0.2 < E_\gamma < 10$ GeV and transverse momentum with respect to the parent muon $p_T < 80$ MeV/c. A good agreement of the observed photon rate with predictions from QED for the muon inner bremsstrahlung was found. The obtained results have to be compared with the observation of the excess of soft photons in hadronic decays of Z^0 reported earlier by DELPHI Collaboration.

Contributed Paper for ICHEP 2006 (Moscow)

1 Introduction

Recent observation of anomalous soft photon production in hadronic events of Z^0 decays collected in the DELPHI experiment at LEP1 [1] has demonstrated the persistence of the soft photon anomaly found earlier in several fixed target experiments with high energy hadronic beams [2-6], this time with a new mechanism of hadron production. The photon kinematic range was defined in [1] as follows: $0.2 < E_\gamma < 1$ GeV, $p_T < 80$ MeV/c, the p_T being the photon transverse momentum with respect to the parent jet direction. The observed soft photon production characteristics were found in [1] to be very close to those reported in [2-6], both for the measured production rate and for the observed ratio of the rate to the inner hadronic bremsstrahlung. The latter was expected to be the main source of the soft photons in kinematic ranges under experimental study [7-9], while the observed signals were found to be several times higher than the bremsstrahlung predictions. No theoretical explanation of this excess is available so far; reviews of the theoretical approaches to the problem can be found in [10, 11] (see also the references [13-33] in [1]).

From the experimental analysis, given a similarity of the soft photon production characteristics in both classes of experiments, the conclusion was drawn that the anomalous (excess) photons are created during the process of hadronization of quarks, i.e. their origin is strictly restricted to a mechanism of hadron production. In such a case a study of photon radiation in a sample of events of pure electroweak origin in the kinematic region close to that explored in [1] becomes highly interesting. This motivated us to study the reaction

$$e^+e^- \to Z^0 \to \mu^+\mu^- n\gamma, \qquad n \geq 1 \tag{1}$$

at LEP1 with the separation of photons in the same kinematic region as in [1] (with the photon transverse momentum being defined now with respect to the parent muon direction). Furthermore, in addition to the low energy (LE) band of $0.2 < E_\gamma \leq 1$ GeV explored in [1], a higher energy (HE) band of $1 < E_\gamma \leq 10$ GeV was involved in the analysis, being restricted however to the photons of small transverse momenta with respect to the muon direction, $p_T < 80$ MeV/c.

Note, the investigation of photon production in $\mu^+\mu^-$ events of Z^0 decays have been done earlier by two of the LEP experiments [12, 13]. However, both these studies aimed at a separation of rather hard photons, isolated from the closest muon. For example, the DELPHI study concerning the final state radiation from muons was restricted to the photon kinematic range of $E_\gamma > 2$ GeV, $\Theta_{\mu\gamma} > 5^\circ$, i.e. to the transverse momenta with respect to the muon, $p_T > 174$ MeV/c.

2 Theoretical predictions for the muon inner bremsstrahlung

The inner bremsstrahlung is a process of the direct photon production via purely QED process. The production rates for the bremsstrahlung from colliding e^+e^- (initial state radiation, ISR) and from final $\mu^+\mu^-$ pairs (final state radiation, FSR) in the p_T range under study can be calculated at once using an universal formula descending from Low [8]:

$$\frac{dN_\gamma}{d^3\vec{k}} = \frac{\alpha}{(2\pi)^2}\frac{1}{E_\gamma}\int d^3\vec{p}_\mu \sum_{i,j}\eta_i\eta_j \frac{-(P_iP_j)}{(P_iK)(P_jK)}\frac{dN_\mu}{d^3\vec{p}_\mu} \tag{2}$$

where K and $\vec{k}$ denote photon four- and three-momenta, P are 4-momenta of beam e^+, e^- and the muon under consideration, and $\vec{p}$ is 3-momentum of the latter; $\eta = 1$ for the beam electron and for μ^+, $\eta = -1$ for the beam positron and for μ^-, and the sum is extended over both beam particles and the muon involved; the last factor in the integrand is a differential muon production rate.

This can be compared to the corresponding formula for the inner hadronic bremsstrahlung in hadronic decays of Z^0:

$$\frac{dN_\gamma}{d^3\vec{k}} = \frac{\alpha}{(2\pi)^2}\frac{1}{E_\gamma}\int d^3\vec{p}_1 ... d^3\vec{p}_N \sum_{i,j}\eta_i\eta_j \frac{-(P_iP_j)}{(P_iK)(P_jK)}\frac{dN_h}{d^3\vec{p}_1 ... d^3\vec{p}_N} \tag{3}$$

where K and $\vec{k}$ denote photon four- and three-momenta, P are 4-momenta of beam e^+, e^- and N charged outgoing hadrons, and $\vec{p}$ are 3-momenta of the latter; $\eta = 1$ for the beam electron and for positive outgoing hadrons, $\eta = -1$ for the beam positron and negative outgoing hadrons, and the sum is extended over all the $N + 2$ charged particles involved; the last factor in the integrand is a differential hadron production rate. Calculations performed with formulae (2,3) show that the bremsstrahlung rate from one muon is approximately equal, in the kinematic region under study, to the bremsstrahlung rate from a hadronic jet of a Z^0 hadronic decay.

The contribution of the ISR to these rates is small being below 2%. The smallness is easy to understand: although the ISR from electron/positron beams is much more intense than the ISR from hadron beams in experiments [2 - 6] where it contributed a significant amount to the detected photon rate, all the extra photons in an experiment with colliding e^+e^- are emitted at very small polar angles with respect to the beam directions, with the angular distribution peaking at $\Theta_\gamma = \sqrt{3}/\Gamma$, where Γ is a beam Lorentz factor ($\Gamma = 0.89 \times 10^5$ at the Z^0 peak), thus yielding few photons in the barrel region used in the analysis. The muon bremsstrahlung radiation has the same angular behaviour, with the Γ being a muon Lorentz factor. The $\Gamma = 402$ for the muons from Z^0 decays which corresponds to the peak position at 4.3 mrad. However due to a fraction of dimuon events entering the analysis at smaller energies owing to the beam initial state radiation, the predicted position of the muon bremsstrahlung peak is shifted to 4.6 mrad. Note, the position of the peak does not depend on the bremsstrahlung photon energy, since the angular and energy dependencies of the produced photon are factorized in f-lae (2,3). The turnover of the muon bremsstrahlung angular distribution at the peak value is termed as the dead cone effect. The observation of the dead cone presents an experimental challenge requiring highly accurate apparatus; the angular resolution of the photon detection which is necessary for the observation of the muon bremsstrahlung dead cone at LEP1 has to be of the order of $1-2$ mrad.

3 Experimental technique

3.1 The DELPHI detector

The DELPHI detector is described in detail elsewhere [14, 15]. The following is a brief description of the subdetector units relevant for this analysis. In the DELPHI reference frame the Z axis is taken along the direction of the e^- beam. The angle Θ is the polar angle defined with respect to the Z-axis, Φ is the azimuthal angle about this axis and R is the distance from this axis.

The TPC, the principal device used in this analysis, was the main tracker of the DELPHI detector; it covered the angular range from 20° to 160° in Θ and extended from 30 cm to 122 cm in R. It provided up to 16 space points for pattern recognition and ionization information extracted from 192 wires.

The identification of muons was based on the muon chambers (MUB) surrounding the barrel region, the hadron calorimeter (HCAL) and the electromagnetic calorimeter (High density Projection Chamber, HPC).

3.2 Identification of soft photons

Photon conversions in front of the main DELPHI tracker (TPC) were reconstructed by an algorithm that examined tracks reconstructed in the TPC. A search was made along each TPC track for points where the tangent of its trajectory points directly to the beam spot in the $R\Phi$ projection. Under the assumption that the opening angle of the electron-positron pair is zero, this point represented a possible photon conversion point at radius R. All tracks which have had a solution R that was more than one standard deviation away from the main vertex, as defined by the beam spot, were considered to be conversion candidates. If two oppositely charged conversion candidates were found with compatible conversion point parameters they were linked together to form the converted photon. The following selection criteria were imposed:

- the Φ difference between the two conversion points was at most 30 mrad;
- the difference between the polar angles Θ of the two tracks was at most 15 mrad;
- at least one of the tracks should have no associated point in front of the reconstructed mean conversion radius.

For the pairs fulfilling these criteria a χ^2 was calculated from $\Delta\Theta$, $\Delta\Phi$ and the difference of the reconstructed conversion radii ΔR in order to find the best combinations in cases where there were ambiguous associations. A constrained fit was then applied to the electron-positron pair candidate which forced a common conversion point with zero opening angle and collinearity between the momentum sum and the line from the beam spot to the conversion point.

The photon detection efficiency, i.e. conversion probability combined with the reconstruction efficiency, was determined with the MC events and tabulated against three variables: E_γ, Θ_γ, (the photon polar angle to the beam) and θ_γ (the photon opening angle to the parent muon). The efficiency varied with the energy from zero at 0.2 GeV up to 4 - 6% at $E_\gamma \geq 1$ GeV, depending on the two other variables.

The accuracy of the converted photon energy measurement was about $\pm 1.2\%$ in the given kinematic range. The angular precision of the photon direction reconstruction was found to be of a Breit-Wigner shape, as expected for the superposition of many Gaussian distributions of varying width [17]. The full widths (Γ's) of the $\Delta\Theta_\gamma$ and $\Delta\Phi_\gamma$ distributions were 5.0 and 4.6 mrad, respectively, in the LE band, and 2.0 and 1.5 mrad in the HE band, with the average of 2.8 ($\Delta\Theta_\gamma$) and 2.4 ($\Delta\Phi_\gamma$) mrad for the combined $0.2 - 10$ GeV interval, thus opening a possibility for the observation of the muon bremsstrahlung dead cone effect.

4 Data selection

4.1 Selection of dimuon events

The data selection was done under standard cuts aimed at the separation of dimuon events which are described below. The consecutive application of the cuts reduced the MC sample of dimuon events produced by DYMU3 generator [18] and passed through the DELPHI detector simulation program DELSIM [14, 15] by factors indicated in parentheses:

- number of charged particles N_{ch} has to be within the interval of $2 \leq N_{ch} \leq 5$, the two of the highest momentum particles must have $p > 15$ GeV/c (0.89);
- the two highest momentum particles have to be within the Θ interval of $20^\circ \leq \Theta \leq 160^\circ$ (0.96);
- the two highest momentum particles must satisfy impact parameter cuts, with the impact parameters being less than 0.2 and 4.5 cm in the $R\Phi$ and Z projections, respectively (0.99);
- no additional charged particles with momenta greater than 10 GeV/c are allowed, except if the fastest particle had a momentum greater than 40 GeV/c (0.999);
- the acollinearity of the two highest momentum particles must be less than 10° (0.99),
- the two highest momentum particles must be identified either as standard, tight or HCAL muons (0.825).

Thus, the total reduction factor for the MC events is 0.69.

Table 1. The data samples used

Sample	1992	1993	1994	1995	Sum
MC generated	124,624	106,449	103,607	116,944	451,624
MC selected	84,863	74,178	76,177	79,056	314,274
RD on DST	498,642	549,018	783,664	451,001	2,282,325
RD selected	25,457	24,007	49,526	23,768	122,758

4.2 Selection of photons

The selection of converted photons was done under the following cuts:

- converted photons with both e^+, e^- arms reconstructed were only considered;
- $20^\circ \leq \Theta_\gamma \leq 160^\circ$;
- 5cm $\leq R_{conv} \leq$ 50cm, where R_{conv} means conversion radius;
- 200 MeV $\leq E_\gamma \leq$ 10 GeV;

383 and 969 converted photons were found under these cuts in the real data (RD) in the two energy bands to be studied: 200 MeV $\leq E_\gamma \leq$ 1 GeV and 1 GeV $\leq E_\gamma \leq$ 10 GeV, respectively.
Of them, 127 and 269 photons are in the selected p_T regions: $p_T < 40$ MeV/c for the LE band and $p_T < 80$ MeV/c for the HE band, respectively.

5 Background

The following background sources were considered:

- External bremsstrahlung:
  The bremsstrahlung radiation from muons when they pass through the material of the experimental setup.
- Secondary photons:
  When a high energy photon generates an e^+e^- pair in the detector material in front of the TPC the pair particles may radiate bremsstrahlung photons, which can enter our kinematic region.
- "Degraded" photons:
  Remnant photons left after a high energy converted photon emitted hard bremsstrahlung.

DELSIM was invoked to reproduce these processes in the MC stream.

Identification of background photons (all dubbed as External Brems) in the MC stream was done under the following criteria:

- absence of a corresponding photon at the event generator level, i.e. in the DYMU3 event record;
- explicit energy loss (>20%) in the case of such a photon being found.

48 and 84 background photons were found in the selected p_T regions: $p_T < 40$ MeV/c for the LE band and $p_T < 80$ MeV/c for the HE band, respectively.

6 Results

The results obtained in this study are presented both uncorrected and corrected for the photon detection efficiency. The exposition of the uncorrected results is motivated by their better statistical and systematic accuracies.

The photon distributions for the θ_γ, p_T and p_T^2 are presented both for the data and the background (left panels of Figs. 1-4), and for their difference (right panels of the figures). The latter is accompanied by the calculated bremsstrahlung distributions shown by triangles.

To quantify the excess of the data over the background the difference between them was integrated in the p_T interval from 0 to 40 MeV/c for the photons of the LE band, and from 0 to 80 MeV/c for the photons of the HE band, and the values obtained were defined as a signal.

6.1 Energy band $0.2 < E_\gamma < 1$ GeV, $p_T < 40$ MeV/c

Photon distributions, uncorrected and corrected for the photon detection efficiency, are displayed in Figs. 1 and 2, respectively. The p_T^2 spectra of the inner muon bremsstrahlung (Figs. 1f, 2f) are fitted by an exponential. The results for the signal rate are the following.

Data uncorrected (corrected) for the detection efficiency:

- RD−Background 0.321±0.050 (20.4±4.1)
- Inner Bremsstrahlung 0.373±0.001 (22.5±0.1)

Thus the predicted and measured muon bremsstrahlung rates agree well (within one standard deviation).

6.2 Energy band $1 < E_\gamma < 10$ GeV, $p_T < 80$ MeV/c

Photon distributions, uncorrected and corrected for the photon detection efficiency, are displayed in Figs. 3 and 4, respectively. The p_T^2 spectra of the inner muon bremsstrahlung (Figs. 3f, 4f) are fitted by an exponential. The results for the signal rate are the following.

Data uncorrected (corrected) for the detection efficiency:

- RD−Background 0.753±0.072 (16.8±2.6)
- Inner Bremsstrahlung 0.773±0.004 (19.4±0.1)

Thus the predicted and measured muon bremsstrahlung rates agree well (within one standard deviation). The smaller values of the corrected experimental and bremsstrahlung rates in the HE energy band as compared to those in the LE band are explained by a higher selectivity of the p_T cut for the higher energy bremsstrahlung photons.

6.3 Observation of the dead cone of the muon bremsstrahlung

The distribution of the photon polar angles with two fine binnings (with 1 and 2 mrad bin widths) are shown in Fig. 5 for the combined sample of the converted photons from the both energy bands, after unfolding the detector angular resolution. The distributions obtained after background subtraction (right panels in Fig. 5) are accompanied

by the calculated bremsstrahlung points. As can be seen from these plots, the experimental points follow well the bremsstrahlung distribution, showing turnover at the predicted bremsstrahlung peak position at 4.6 mrad. This means the dead cone observation, which enriches the agreement between the experimental findings of the inner muon bremsstrahlung characteristics reported in this note, and the QED predictions for the process.

7 Conclusions

This analysis shows a good agreement of the observed photon production rate with the QED predictions for the muon inner bremsstrahlung in events of $\mu^+\mu^-$ decays of the Z^0. This indicates that the phenomenon of anomalous soft photons observed in [1-6] seems to be restricted to reactions of multiple hadron production.

The bremsstrahlung dead cone is observed for the first time in measuring the direct photon production in high energy experiments, also being in a good agreement with the predicted bremsstrahlung behaviour.

References

[1] DELPHI Collaboration, J. Abdallah et al., CERN-PH-EP-2005-052, hep-ex/0604038 (to appear in Eur.Phys.J. C)

[2] P.V. Chliapnikov et al., Phys. Lett. B **141**, 276 (1984)

[3] F. Botterweck et al., Z. Phys. C **51**, 541 (1991)

[4] S. Banerjee et al., Phys. Lett. B **305**, 182 (1993)

[5] A. Belogianni et al., Phys. Lett. B **408**, 487 (1997)
A. Belogianni et al., Phys. Lett. B **548**, 122 (2002)

[6] A. Belogianni et al., Phys. Lett. B **548**, 129 (2002)

[7] L.D. Landau, I.Ya. Pomeranchuk, Dokl. Akad. Nauk SSSR **92**, 535, 735 (1953) (Papers No. 75 and 76 in the English edition of L.D. Landau collected works)

[8] F. Low, Phys. Rev. **110** , 974 (1958)

[9] V.N. Gribov, Sov. J. Nucl. Phys. **5**, 280 (1967)

[10] V. Balek, N. Pišútová and J. Pišút, Acta Phys. Pol. B **21**, 149 (1990)

[11] P. Lichard, Phys. Rev. D **50**, 6824 (1994)

[12] OPAL Collaboration, D.P. Acton et al., Phys. Lett B **273** 338 (1991)

[13] DELPHI Collaboration, P. Abreu et al., Z. Physik C **65** 603 (1995).

[14] DELPHI Collaboration, P. Aarnio et al., Nucl. Instr. and Meth. A **303**, 233 (1991)

[15] DELPHI Collaboration, P. Abreu et al., Nucl. Instr. and Meth. A **378**, 57 (1996)

[16] DELPHI Collaboration, W. Adam et al., Z. Phys. C **69**, 561 (1996)

[17] W.T. Eadie et al., *Statistical Methods in Experimental Physics* (North-Holland, Amsterdam, 1982) p. 90

[18] J.E. Campagne, R. Zitoun, Z. Phys. C **43**, 469 (1989)
J.E. Campagne et al. in: Z Physics at LEP1, G. Altarelli, R. Kleiss and C. Verzegnassi eds., CERN Yellow Report No.89-08, 1989, vol.3, 2.2.5, 3.2.5

DELPHI

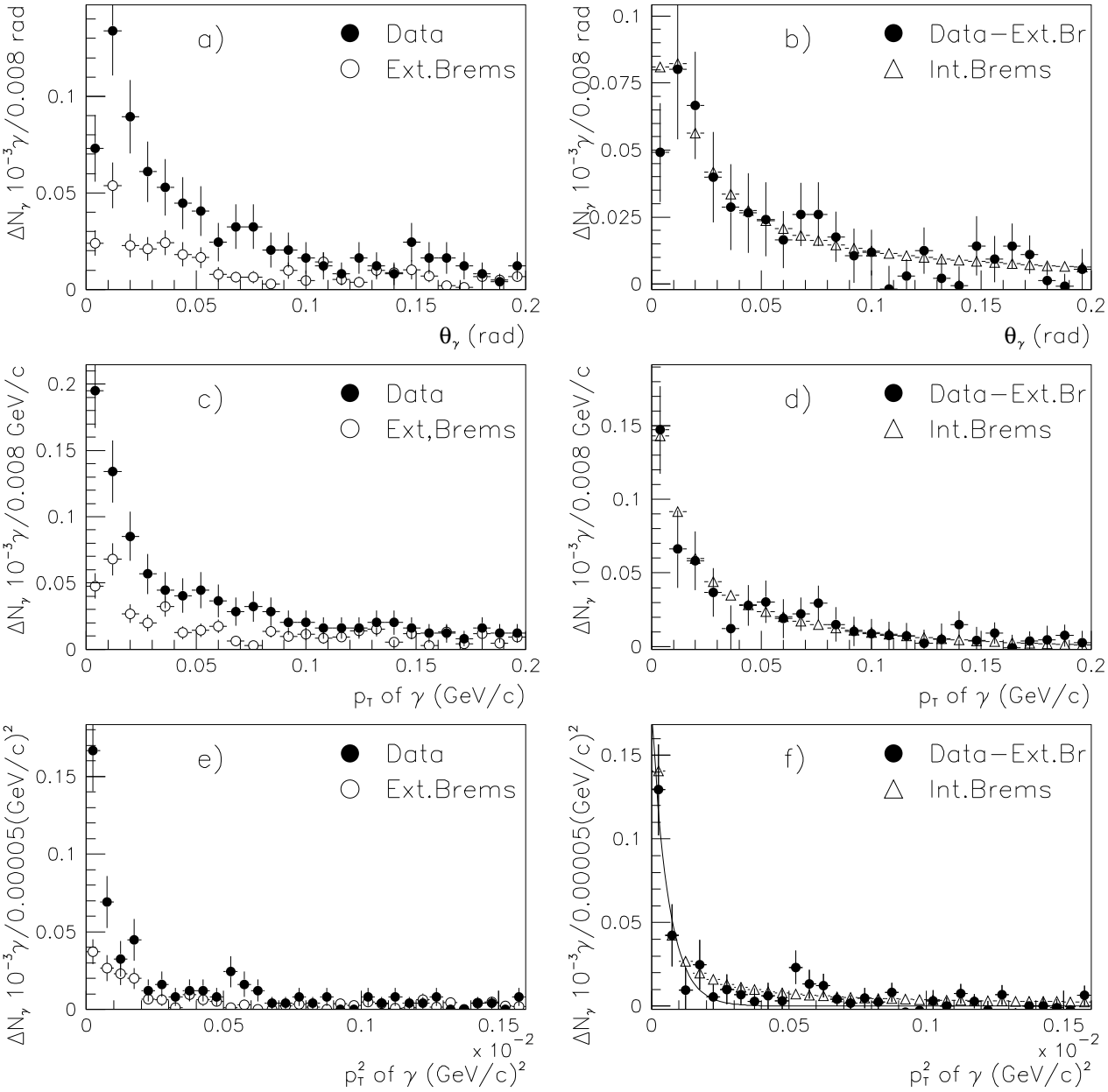

Figure 1: Photon distributions in the photon energy band $0.2 < E_\gamma < 1$ GeV uncorrected for the photon detection efficiency. Left panels: the data and background distributions for a) θ_γ (photon polar angle relative to the parent jet direction); c) photon p_T; e) photon p_T^2. Right panels, b), d), f): the difference between the data and background for the same variables, respectively. "Ext.Brems" corresponds to the background, "Int.Brems" corresponds to the inner hadronic bremsstrahlung predictions. The errors are statistical. The curve in fig. 1f) is the fit by an exponential.

DELPHI

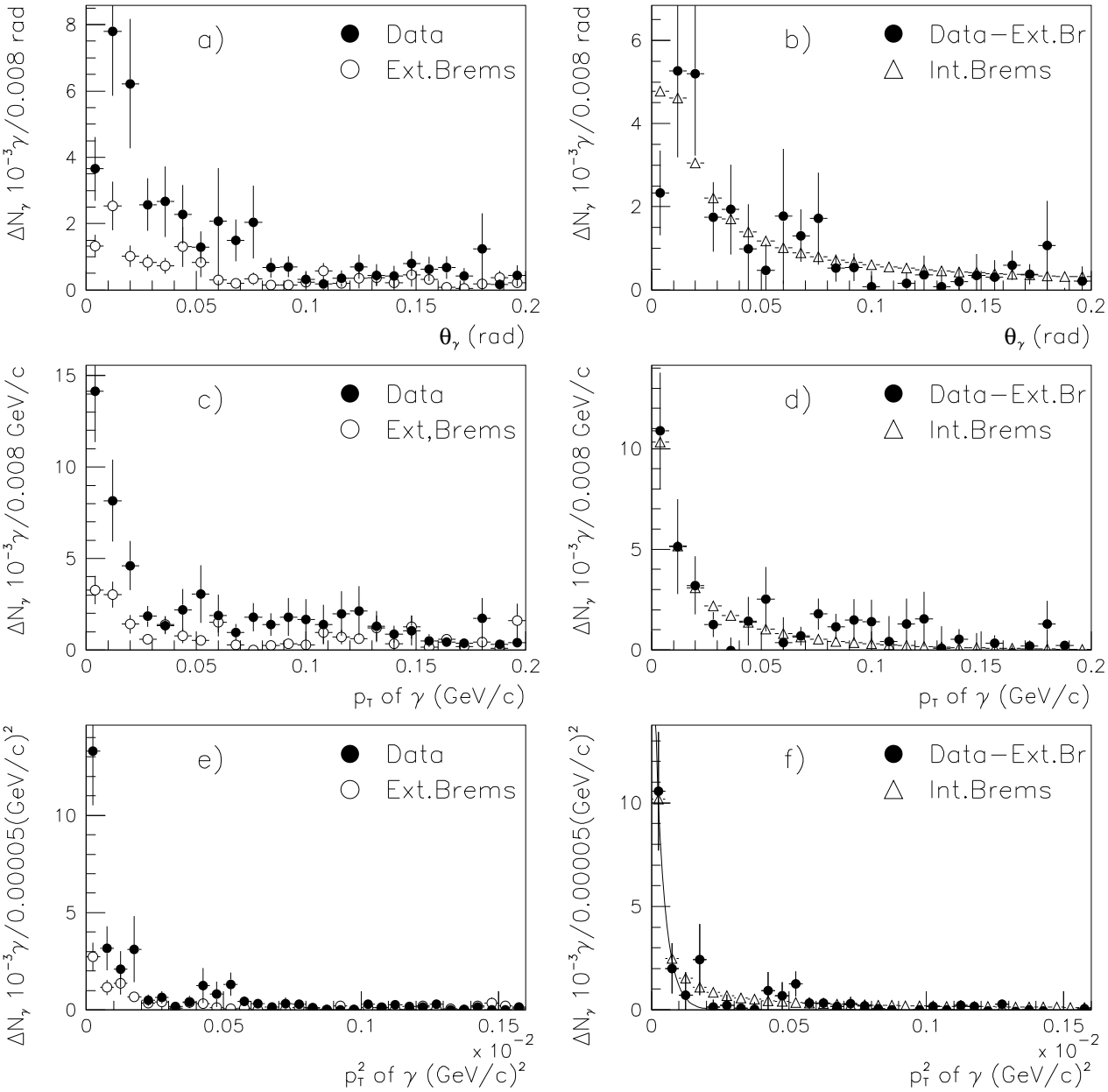

Figure 2: The same as in fig. 1, corrected for the efficiency of photon detection.

DELPHI

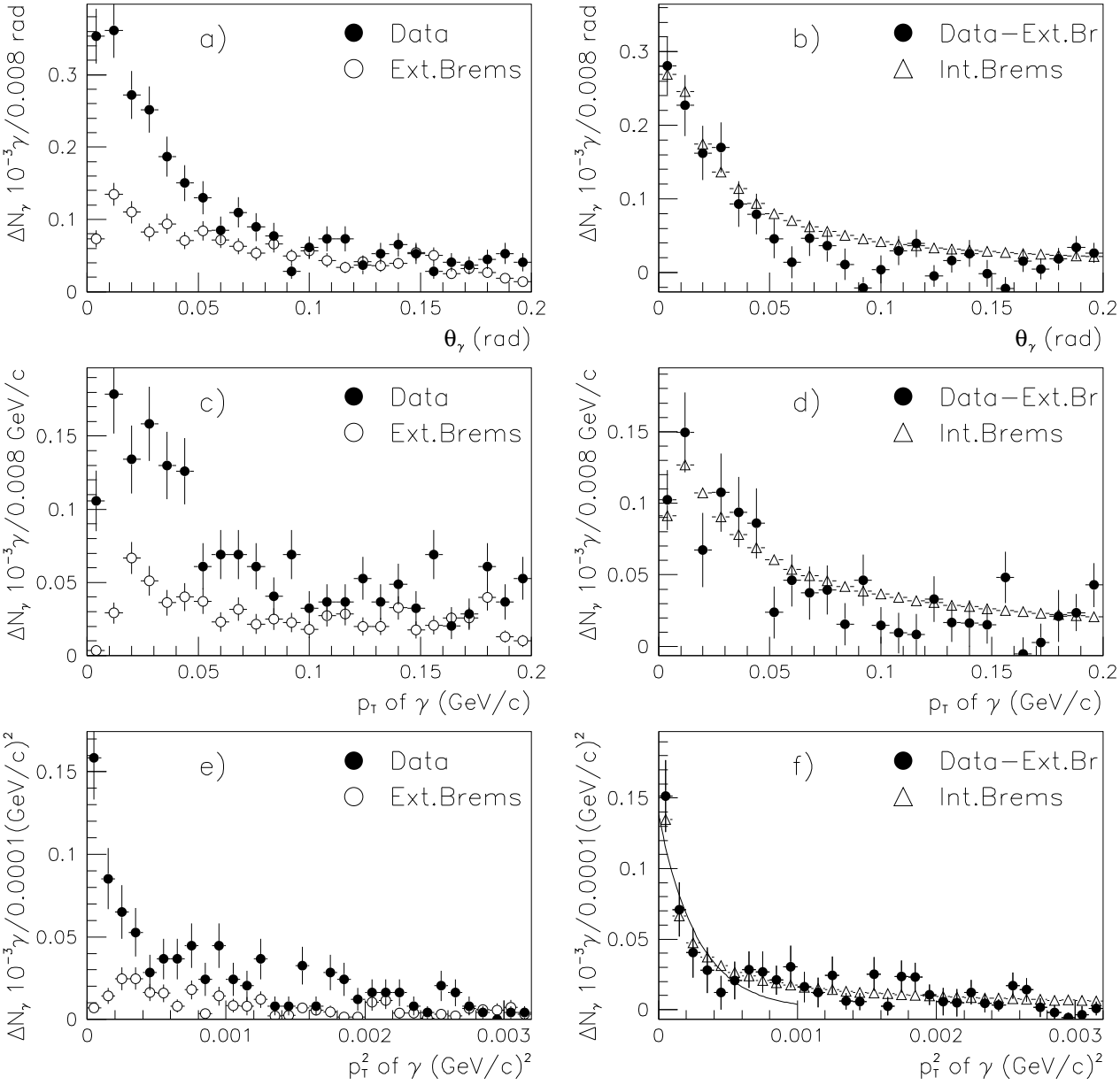

Figure 3: Photon distributions in the photon energy band $1 < E_\gamma < 10$ GeV uncorrected for the photon detection efficiency. Left panels: the data and background distributions for a) θ_γ (photon polar angle relative to the parent jet direction); c) photon p_T; e) photon p_T^2. Right panels, b), d), f): the difference between the data and background for the same variables, respectively. The errors are statistical. The curve in fig. 3f) is the fit by an exponential.

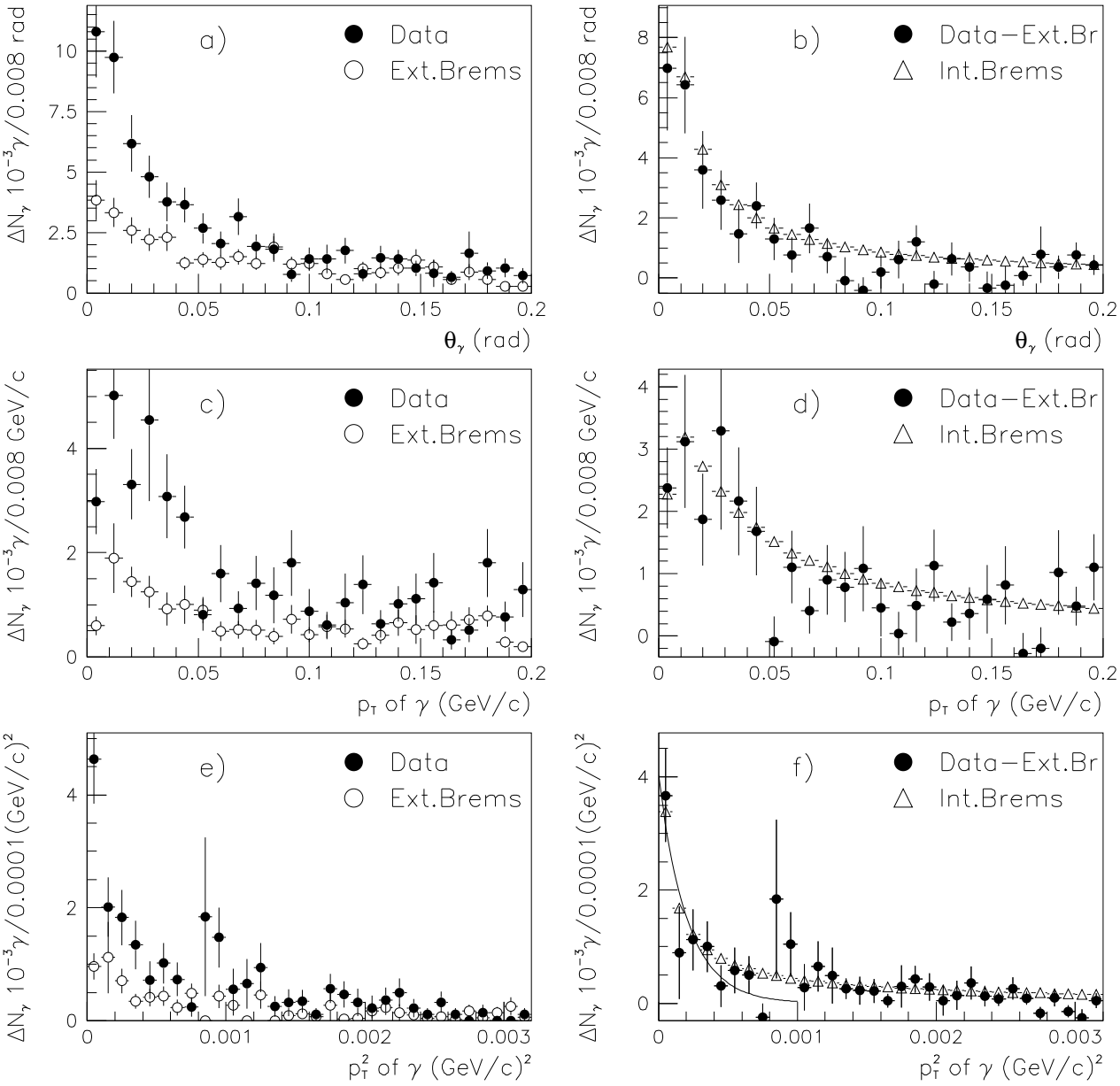

Figure 4: The same as in fig. 3, corrected for the efficiency of photon detection.

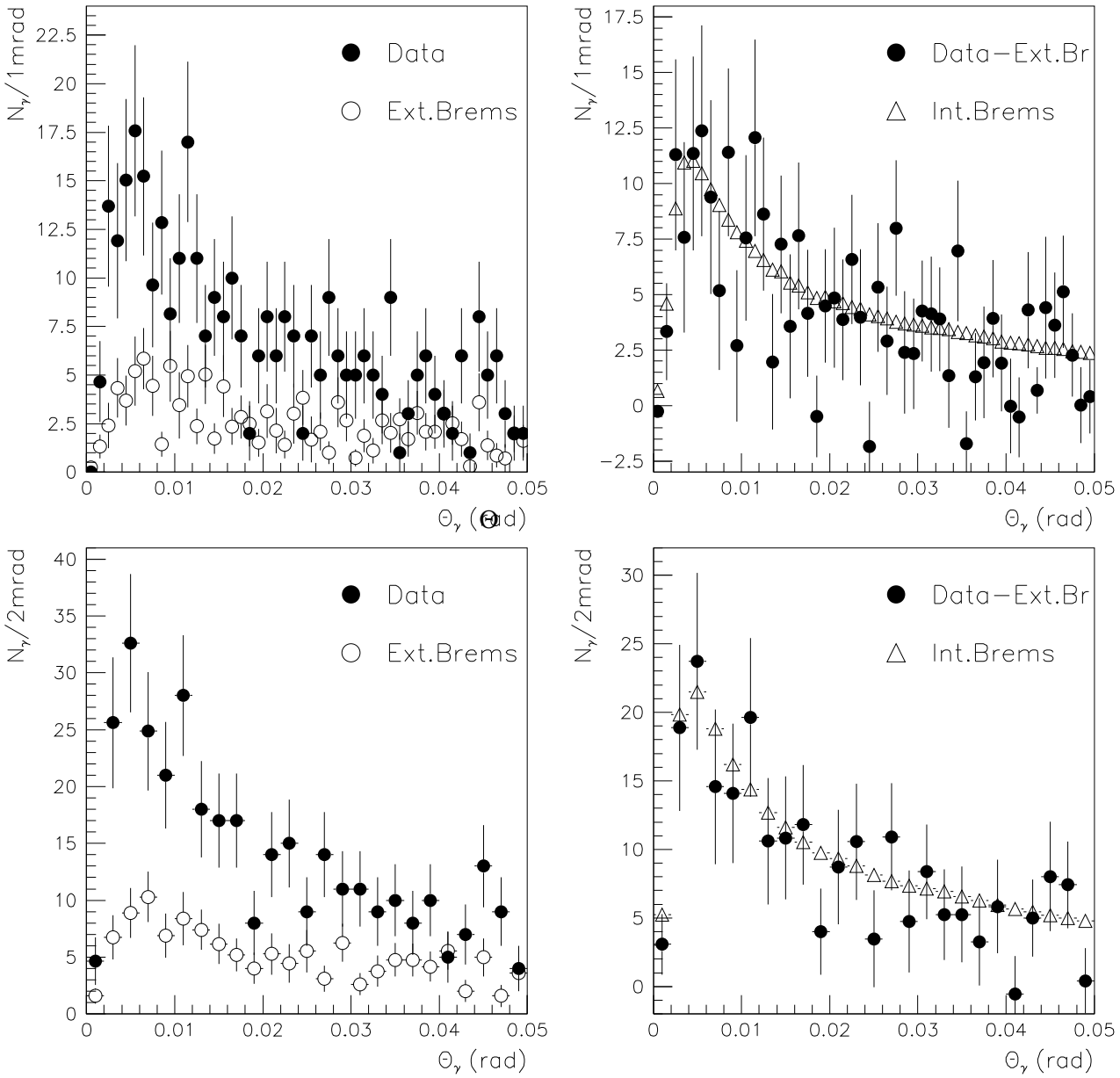

Figure 5: Dead cone of bremsstrahlung radiation as seen in the photon polar angle distributions. Upper panels: with 1 mrad bin width in θ_γ. Bottom panels: with 2 mrad bin width.